Short Communication

Institution of MECHANICAL ENGINEERS

Journal of ENGINEERING MANUFACTURE

Proc IMechE Part B:
J Engineering Manufacture
1–6

DOI: 10.1177/0954405417716955
journals.sagepub.com/home/pib
SAGE

Line-of-sight rate modeling and error analysis of inertial stabilized platforms by coordinate transformation

Qingjia Gao[1,2], Qiang Sun[1], Feng Qu[1], Jiang Wang[1], Xizhen Han[1] and Jian Zhao[3]

Abstract

Line-of-sight rate is the key parameter that enables inertial stabilized platforms to implement guidance laws successfully for target tracking or attacking. It is always obtained by experiments. In this article, a theoretical model of the line-of-sight rate is established for the first time, starting with the gimbal motion. The strategy to acquire line-of-sight rate is based on the servo control circuit. The measurement equations for line-of-sight rate are derived using a coordinate transformation. An error model is then obtained with the help of differentiation. The error of an inertial stabilized platform prototype is measured, showing that the line-of-sight rate error can be predicted accurately. Finally, a high-precision inertial stabilized platform is successfully designed and analyzed, with the accuracy of 0.06°/s and 0.37°/s when line-of-sight rates are set to 1.5°/s and 9°/s, respectively.

Keywords

Line-of-sight rate, inertial stabilized platforms, modeling, coordinate transformation

Date received: 28 February 2017; accepted: 21 May 2017

Introduction

Recently, inertial stabilized platforms (ISPs) have been usually installed in unmanned air vehicles or missiles in order to track or attack targets, which is of great significance in scientific, military, and commercial applications.[1–3] ISPs mainly include optical imaging system and stabilized frame. They should provide rapid and accurate rate tracking of the line-of-sight (LOS) error signals generated by the imaging sensor located in the inner gimbal.[1,4] In the stabilization loop, they are utilized to keep the stability of the LOS, which is the displacement vector of the target with respect to the inertial space reference system; therefore, the carrier disturbance can be attenuated, and clear target images are obtained.[5,6] In the track loop, the LOS rate, as a key signal, reflects the target motion information relative to the missile in real time. It is filtered and output for use in guidance law implementation.[7,8] The typical configuration is illustrated in Figure 1. Hence, the accuracy of LOS and its rate both significantly affect the target tracking and attacking. It is necessary to model and decrease these errors to further improve system performance.

There are currently many approaches to establishing the error model of ISPs location pointing accuracy to guarantee LOS stability, such the Debye–Huckel equation,[9,10] quaternions,[5] coordinate transformation,[11,12] and multi-body kinematics theory.[13] These approaches form the main basis for acquiring clear target images. Studies about LOS rate mainly focus on its estimation methods, such as the Kalman filter,[14] two-stage observer,[15] and disturbance observer-based techniques,[16] which effectively improve signal-to-noise ratio by signal processing. However, the original errors of the LOS rate cannot be analyzed and controlled. With the target position not known in real time, the LOS rate is always obtained by experiments because it cannot be mathematically calculated directly from the system sensor. Hence, it is not only an appropriate estimation method needed to improve signal quality, but it is also

[1]Changchun Institute of Optics, Fine Mechanics and Physics, Chinese Academy of Sciences, Changchun, China
[2]University of Chinese Academy of Sciences, Beijing, China
[3]Suzhou Institute of Biomedical Engineering and Technology, Chinese Academy of Sciences, Suzhou, China

Corresponding author:
Qingjia Gao, Changchun Institute of Optics, Fine Mechanics and Physics, Chinese Academy of Sciences, No. 3888, Dong Nanhu Road, Jingkai District, Changchun 130033, China.
Email: gaoqj@ciomp.ac.cn

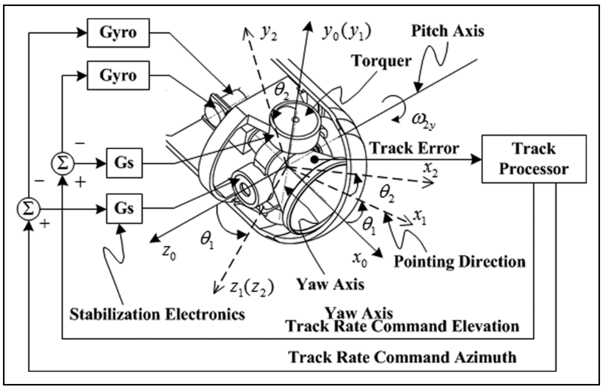

Figure 1. Two-axis tracker configuration.

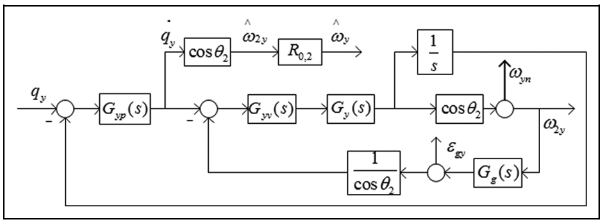

Figure 2. Detailed structure of the servo control system for the yaw circuit.

necessary to model the original error of LOS rate in theory so as to guarantee sufficient precision before signal processing.

In this article, a theoretical model of the LOS rate is presented for the first time. Restraining factors are calculated in detail. Error analysis and measurement for an ISP prototype is also carried out.

LOS rate modeling

Acquiring principle

To lower the system noise as much as possible, the LOS rate is acquired from the servo control circuit. Its structure for the yaw circuit is shown in Figure 2, in which the torque observer is neglected. Here, q_y is the expected LOS angle in the gimbal base frame, $\dot{q}_y$ is the estimated LOS rate, $\hat{\omega}_{2y}$ is the actual LOS rate in the LOS coordinate system, $G_{yp}(s)$ is the position loop controller, $G_{yv}(s)$ is the velocity loop controller, $G_y(s)$ is the controlled object, and $G_g(s)$ is the transfer function of the gyro.

The transfer function from LOS angle to LOS rate is given by

$$\frac{\dot{q}_y(s)}{q_y(s)} = \frac{G_{yp}(s)}{1 + G_{yp}(s)\frac{G_{yv}(s)G_y(s)}{1 + sG_{yv}(s)G_y(s)}} \tag{1}$$

The yaw LOS rate in LOS axial coordinates is then acquired by means of a certain frequency sampling of $\hat{\omega}_{2y}$. Finally, the yaw LOS rate in the gimbal coordinate system can be obtained by coordinate transformation.

Error model of the LOS rate

Referring to Figure 1, three coordinate systems are used to define gimbal motion, starting with the gimbal base frame (o-$x_0y_0z_0$), followed by the gimbal outer frame (o-$x_2y_2z_2$), and finally the gimbal inner frame (o-$x_1y_1z_1$). The oy_1 and oz_2 axes are coincident with yaw axis and pitch axis, respectively, while ox_1 parallels the pointing direction. Furthermore, θ_1 is the yaw angle and θ_2 is the pitch angle. The coordinate transforms between o-$x_1y_1z_1$ and o-$x_0y_0z_0$ and between o-$x_2y_2z_2$ and o-$x_1y_1z_1$ are written as

$$\begin{aligned} R_{0,1}(\theta_1) &= \begin{bmatrix} C\theta_1 & 0 & S\theta_1 \\ 0 & 1 & 0 \\ -S\theta_1 & 0 & C\theta_1 \end{bmatrix} \text{ and } R_{1,2}(\theta_2) \\ &= \begin{bmatrix} C\theta_2 & -S\theta_2 & 0 \\ S\theta_2 & C\theta_2 & 0 \\ 0 & 0 & 1 \end{bmatrix} \end{aligned} \tag{2}$$

where $C\theta$ expresses the function of $\cos\theta$ and $S\theta$ expresses the function of $\sin\theta$.

Let the LOS rate of yaw and pitch in the gimbal base frame be defined by $\hat{\omega}_y$ and $\hat{\omega}_z$, respectively. The relationship of the LOS rate between the gimbal frame and LOS axis is given by

$$\begin{bmatrix} \times \\ \hat{\omega}_y \\ \hat{\omega}_z \end{bmatrix} = R_{0,2}(\theta_1)\begin{bmatrix} \times \\ \hat{\omega}_{2y} \\ \hat{\omega}_{2z} \end{bmatrix} = R_{0,1}(\theta_1)R_{1,2}(\theta_2)\begin{bmatrix} \times \\ \hat{\omega}_{2y} \\ \hat{\omega}_{2z} \end{bmatrix} \tag{3}$$

Then, the measurement equations of $\hat{\omega}_y$ and $\hat{\omega}_z$ can be written as

$$\hat{\omega}_y = \hat{\omega}_{2y}C\theta_2 \tag{4}$$

$$\hat{\omega}_z = \hat{\omega}_{2y}S\theta_1S\theta_2 + \hat{\omega}_{2z}C\theta_1 \tag{5}$$

In the process of coordinate transformation, it is clear that the angle errors caused by the encoder and mechanical installation inevitably affect LOS rate accuracy. In other words, the angle errors produce a main effect on the yaw and pitch rotation angle.

Assume that LOS rate errors and rotation angles are all independent random variables, and let the standard deviation be expressed as σ. With the help of differentiation, then, the standard deviation of the LOS rate for yaw and pitch in the gimbal coordinate system are, respectively, given by

$$\sigma_{\Delta\hat{\omega}_y} = \left(C^2\theta_2\sigma^2_{\Delta\hat{\omega}_{2y}} + \hat{\omega}^2_{2y}S^2\theta_2\sigma^2_{\Delta\theta_2}\right)^{1/2} \tag{6}$$

and

$$\begin{aligned} \sigma_{\Delta\hat{\omega}_z} = \Big(&S^2\theta_1S^2\theta_2\sigma^2_{\Delta\hat{\omega}_{2y}} + C^2\theta_1\sigma^2_{\Delta\hat{\omega}_{2z}} \\ &+ \left(\hat{\omega}^2_{2y}C^2\theta_1S^2\theta_2 + \hat{\omega}^2_{2z}S^2\theta_1\right)\sigma^2_{\Delta\theta_1} \\ &+ \hat{\omega}^2_{2y}S^2\theta_1C^2\theta_2\sigma^2_{\Delta\theta_2}\Big)^{1/2} \end{aligned} \tag{7}$$

where $\sigma_{\Delta\hat{\omega}_{2y}}$ and $\sigma_{\Delta\hat{\omega}_{2z}}$ are the standard deviations of the yaw and pitch LOS rate errors in LOS axis coordinates, respectively. The rotation angle error of the yaw axis, defined by $\Delta\theta_1$, consists of encoder error $\Delta\theta_{11}$ and mechanical installation error $\Delta\theta_{12}$. We have the relationship $\Delta\theta_1 = \Delta\theta_{11} + \Delta\theta_{12}$. In a similar way, it can be shown that the rotation angle error of the pitch axis $\Delta\theta_2$ can be written as $\Delta\theta_2 = \Delta\theta_{21} + \Delta\theta_{22}$.

Error analysis and calculation

Gyroscope error

There is a direct effect of the gyro error on the LOS rate. Based on the principle of LOS rate acquisition, the transfer function from the gyro error to the LOS rate for yaw in the LOS axis coordinate system is given by

$$\frac{\dot{q}_y}{\varepsilon_{gy}} = \frac{G_{yp}(s)G_{yv}(s)G_y(s)}{(1 + G_{yv}(s)G_y(s))s + G_{yp}(s)G_{yv}(s)G_y(s)} \tag{8}$$

If we let the standard deviations of the gyro error for yaw and pitch be defined by σ_{gy} and σ_{gp}, respectively, they have the following relationship

$$\sigma_{gy} = \sigma_{gp} = \sigma_g \tag{9}$$

Referring to the transfer function of the gyro error, we have the following standard deviations of yaw and pitch in the gimbal coordinate system

$$\sigma_{\dot{q}_y} = \sigma_{\dot{q}_p} = \sigma_{\dot{q}} \tag{10}$$

Consequently, according to the principle of LOS rate acquisition, the standard deviations of the LOS rate for yaw and pitch in the LOS axis coordinate system are, respectively, given by

$$\sigma_{\Delta\hat{\omega}_{2y}} = \sigma_{\dot{q}} \cos\theta_2 \tag{11}$$

and

$$\sigma_{\Delta\hat{\omega}_{2z}} = \sigma_{\dot{q}} \tag{12}$$

Encoder angle error

Assume that the same kind of encoder is adopted. Then, the standard deviations of the rotation angle for yaw and pitch caused by encoder, respectively, defined by $\sigma_{\Delta\theta_{11}}$ and $\sigma_{\Delta\theta_{21}}$, can be equal, that is

$$\sigma_{\Delta\theta_{11}} = \sigma_{\Delta\theta_{11}} = \sigma_{\Delta\theta} \tag{13}$$

Mechanical installation errors

The axis rotation is always non-ideal in the process of mechanical design and assemblies; hence, mechanical installation errors are inevitable for both yaw and pitch axes. Let the standard deviations of yaw and pitch be defined by $\sigma_{\Delta\theta_{12}}$ and $\sigma_{\Delta\theta_{22}}$, respectively. Referring to Figure 3, angular error $\Delta\theta_{12}$ of the yaw axis is composed of mechanical installation errors with respect to the pitch and LOS axes. Similarly, angular error $\Delta\theta_{22}$ of the pitch axis is composed of mechanical errors with respect to the yaw and LOS axes.

Angular errors in the yaw axis mainly consist of five components, as shown in Figure 4(a), where $\Delta\theta_{121}$ is the yaw angular error caused by the outer frame installation, $\Delta\theta_{122}$ is the yaw angular error caused by the LOS axis installation, $\Delta\theta_{123}$ is the yaw angular error caused by coaxiality, $\Delta\theta_{124}$ is the yaw angular error caused by the installation clearance of the pitch axis, and $\Delta\theta_{125}$ is the yaw angular error caused by the bearing structure of the pitch.

Therefore, the total yaw angular error defined $\Delta\theta_{12}$ can be written as

$$\Delta\theta_{12} = \Delta\theta_{121} + \Delta\theta_{122} + \Delta\theta_{123} + \Delta\theta_{124} + \Delta\theta_{125} \tag{14}$$

Assume these angular errors are all random variables and independent of each other. Then, $\Delta\theta_{121}$, $\Delta\theta_{122}$, and $\Delta\theta_{123}$ are all treated as system errors, and $\Delta\theta_{124}$ and $\Delta\theta_{125}$ are considered to be random errors. As a result, the standard deviation of the yaw angular error caused by mechanical installation is summarized by

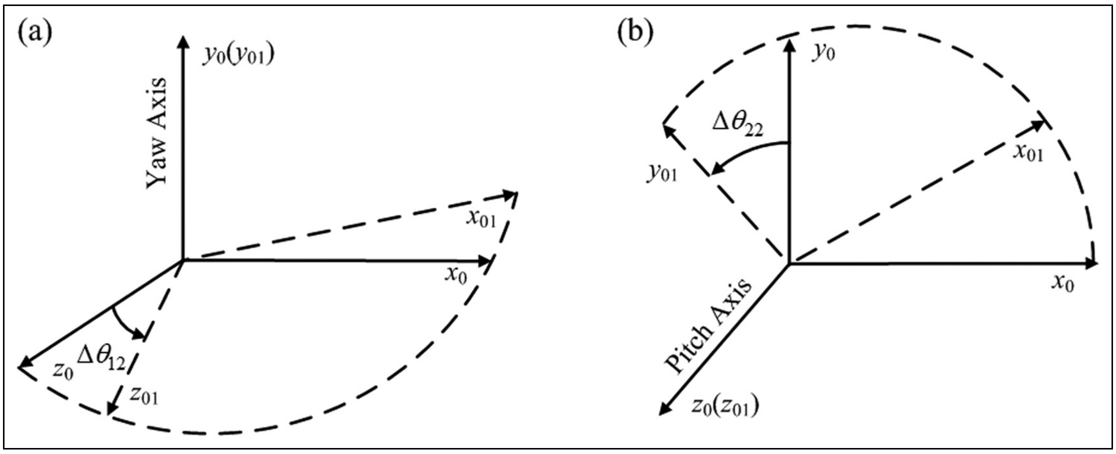

Figure 3. Influence of angular position on axis error: (a) mechanical installation error of pitch and LOS axes and (b) mechanical installation error of yaw and LOS axes.

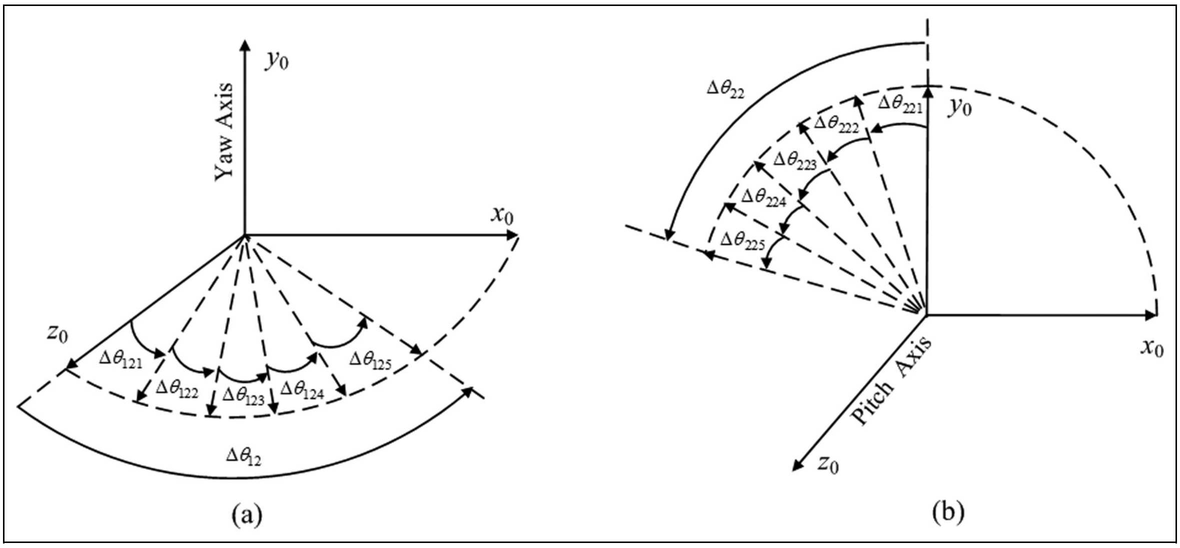

Figure 4. Composition of the angular error in (a) yaw and (b) pitch directions.

$$\sigma_{\Delta\theta_{12}} = k_{s1}(\sigma^2_{\Delta 121} + \sigma^2_{\Delta 122} + \sigma^2_{\Delta 123})^{1/2} + k_{r1}(\sigma^2_{\Delta 124} + \sigma^2_{\Delta 125})^{1/2} \tag{15}$$

The composition of the pitch angular error is shown in Figure 4(b). Similarly, the standard deviation of the pitch angular error caused by mechanical installation can be summarized by

$$\sigma_{\Delta\theta_{22}} = k_{s2}(\sigma^2_{\Delta 221} + \sigma^2_{\Delta 222} + \sigma^2_{\Delta 223})^{1/2} + k_{r2}(\sigma^2_{\Delta 224} + \sigma^2_{\Delta 225})^{1/2} \tag{16}$$

Experiment and results

We consider an ISP prototype with an operating range of 2000 m, a maximum LOS rate of 9°/s, and a frame angle of ±20° as an example. Furthermore, it has the characteristics of seventh-level machining precision and P4-level bearings. The mechanical installation error data used for calculation are listed in Table 1.

The experimental apparatus, shown in Figure 5, is made up of a precise five-axis turntable, an ISP prototype, an IR target simulator, and a data acquisition and control system. The ISP was installed in the roll axis, which is the inner three-axis frame of the turntable, and the IR simulator was placed in the pitch axis, which is the outer two-axis frame of the turntable. Prior to the experiment, it was necessary to align the reticule of the IR imager with that of the simulator by adjusting the angular position of the three-axis frame. In the experiment, keeping the ISP fixed, the IR target moved through the field of view of the ISP at a uniform angular velocity with a given value. Finally, the error of the LOS rate was obtained by means of data processing.

According to the system specifications and to save costs, a Micro Electro Mechanical System (MEMS) gyro with two axes (STIM210, σ = 0.067°/s) and magnetic encoder (σ = 0.05°) were adopted for the first generation prototype.Figure 6 shows the calculation errors between simulation and measurement results, with a maximum error of 6.5%. Therefore, the LOS rate model has enough accuracy for engineering design.

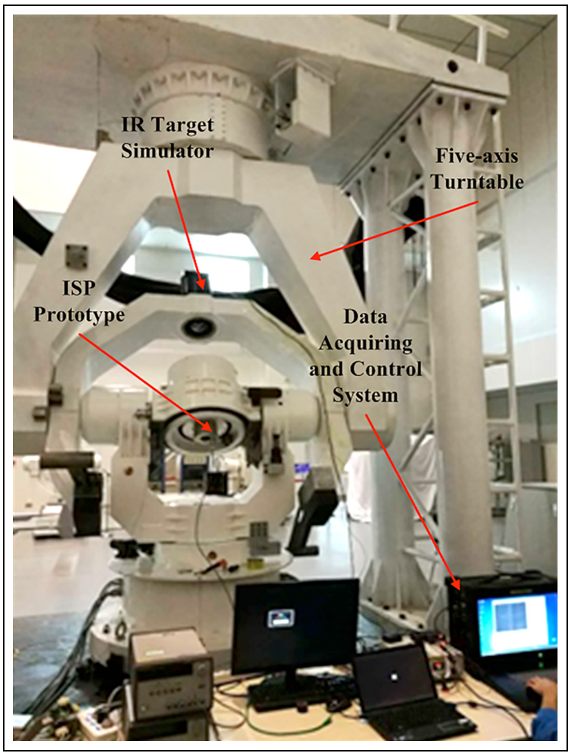

Figure 5. Experimental apparatus for measuring LOS rate error.

Using the LOS rate model, a new ISP is designed and analyzed. The major technical indexes about LOS rate are that the precision is superior to 0.1°/s and 0.4°/s, when the LOS rate is set to 1.5°/s and 9°/s, respectively. After detailed calculation, the seventh-level machining precision and P4-level bearings are adopted, and a flexible gyro (σ = 0.033°/s) and 16-bit optical-electricity

Table 1. Error values used in the calculation and experiment.

Order	Error description	Error distribution	Error value (°)
1	Yaw angular error caused by the outer frame installation	Uniform	$\sigma_{\Delta 121}=2.20\times 10^{-3}$
2	Yaw angular error caused by the LOS axis installation	Uniform	$\sigma_{\Delta 122}=5.51\times 10^{-3}$
3	Yaw angular error caused by coaxiality	Uniform	$\sigma_{\Delta 123}=7.33\times 10^{-3}$
4	Yaw angular error caused by the pitch axis installation clearance	Uniform	$\sigma_{\Delta 124}=2.99\times 10^{-3}$
5	Yaw angular error caused by the pitch bearing structure	Uniform	$\sigma_{\Delta 125}=5.96\times 10^{-3}$
6	Pitch angular error caused by the outer frame installation	Uniform	$\sigma_{\Delta 221}=2.20\times 10^{-3}$
7	Pitch angular error caused by LOS axis installation	Uniform	$\sigma_{\Delta 222}=5.51\times 10^{-3}$
8	Pitch angular error caused by coaxiality	Uniform	$\sigma_{\Delta 223}=6.02\times 10^{-3}$
9	Pitch angular error caused by the yaw axis installation clearance	Uniform	$\sigma_{\Delta 224}=3.16\times 10^{-3}$
10	Pitch angular error by the yaw bearing structure	Uniform	$\sigma_{\Delta 225}=5.96\times 10^{-3}$

LOS: line of sight.

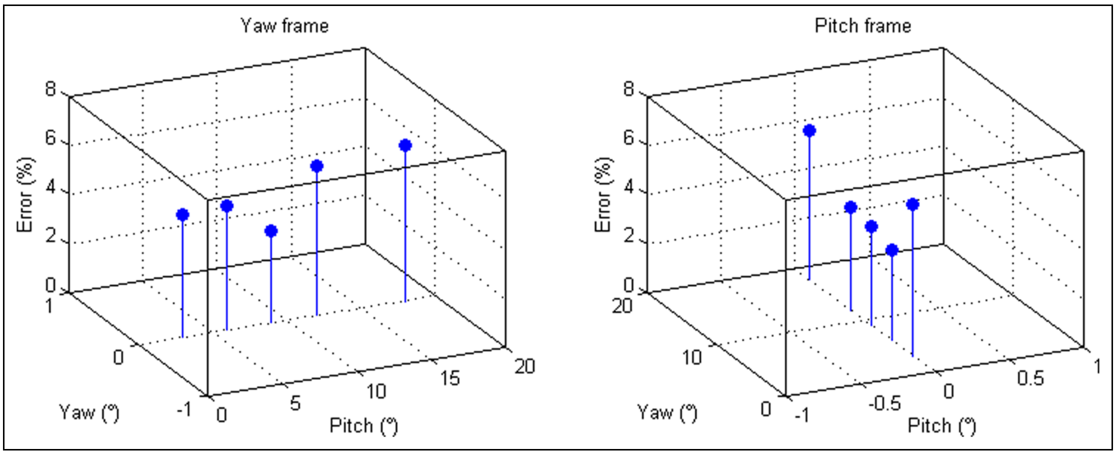

Figure 6. The calculation errors between simulation and measurement results.

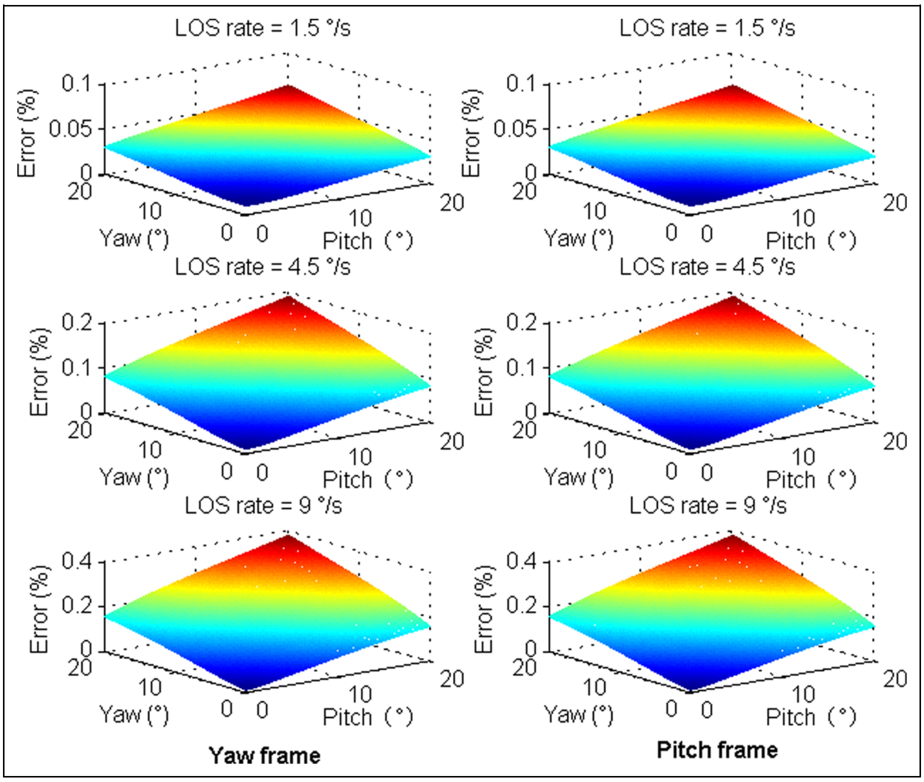

Figure 7. Calculation results at different LOS rates and frame angles for yaw and pitch.

encoder ($\sigma = 0.005°$) are adopted based on a comprehensive consideration of the manufacturing, device cost, and practicality.

Figure 7 shows the calculation results at different LOS rates and frame angles for yaw and pitch. We can see that the LOS rate errors tend to increase as the LOS rate or frame angle increases. Furthermore, greater LOS rates lead to a larger error curve slope. Additionally, as the LOS rate and frame angle increase, the slope of the error curve becomes smaller than that of lower precision sensors. Finally, when the LOS rates are set to 1.5°/s and 9°/s with the maximum frame angle of 20°, the yaw and pitch LOS rate errors at the three sigma level are below 0.06°/s and 0.37°/s, respectively. As a result, the design specifications are satisfied in the whole design frequencies.

Conclusion

The LOS rate is the major parameter that enables the ISP to autonomously track or attack a target. Starting with the characteristics of the system structure, a theoretical model of the LOS rate is presented in this article. The error analysis and measurement for an ISP prototype was carried out with the maximum error of 6.5%. As the LOS rate or frame angle increases, the errors also tend to increase. Furthermore, greater LOS rates lead to larger error curve slope. A high-precision ISP is designed and analyzed using the LOS rate model, with the accuracy of 0.06°/s and 0.37°/s when LOS rates are set to 1.5°/s and 9°/s, respectively. The LOS rate model has enough accuracy for engineering design.

Declaration of conflicting interests

The author(s) declared no potential conflicts of interest with respect to the research, authorship, and/or publication of this article.

Funding

The author(s) disclosed receipt of the following financial support for the research, authorship, and/or publication of this article: This work was supported by the National Natural Science Foundation of China (Grant No. 11372309 and 61304017) and Stage III of the Knowledge Innovation Program of the Chinese Academy of Sciences (Grant No. YYYJ-1122).

References

1. Hilkert JM. Inertially stabilized platform technology concepts and principles. *IEEE Contr Syst Mag* 2008; 28: 26–46.
2. Tang QJ, Wang XJ and Yang QP. Static pointing error analysis of electro-optical detection systems. *Proc IMechE, Part B: J Engineering Manufacture* 2016; 230: 593–600.
3. Zhou XY, Lu YF, Zhang ZY, et al. Error analysis and calibration of gyro-stabilized platform for electro-optical pointing system. *Appl Mech Mater* 2012; 141: 264–269.
4. Waldmann J. Line-of-sight rate estimation and linearizing control of an imaging seeker in a tactical missile guided by proportional navigation. *IEEE T Contr Syst T* 2002; 10: 556–567.
5. Tang QJ, Wang XJ, Yang QP, et al. Calibration error analysis of inertially stabilized platforms using quaternions and octonions in rotation decomposition. *Proc IMechE, Part B: J Engineering Manufacture* 2016; 230: 1771–1774.
6. Tian J, Yang WS, Peng ZM, et al. Inertial sensor-based multiloop control of fast steering mirror for line of sight stabilization. *Opt Eng* 2016; 55: 111602.
7. Dhananjay N, Lum KY and Xu JX. Proportional navigation with delayed line-of-sight rate. *IEEE T Contr Syst T* 2013; 21: 247–253.
8. Song SH. A LOS rate estimation method for bank-to-turn missiles. *IEEE T Aero Elec Sys* 2008; 44: 1599–1608.
9. Sladek J, Ostrowska K and Gaska A. Modeling and identification of errors of coordinate measuring arms with the use of a metrological model. *Measurement* 2013; 46: 667–679.
10. Hong HJ, Zhou XY, Zhang ZY, et al. Modeling and calibration of pointing errors using a semi-parametric regression method with applications in inertially stabilized platforms. *Proc IMechE, Part B: J Engineering Manufacture* 2013; 227: 1492–1503.
11. Wang JQ, Jin G and Yan CX. Orientation error analysis of airborne opto-electric tracking and measuring device. *Optic Precis Eng* 2005; 13: 105–116 (in Chinese).
12. Wang J, Gao LM and Yao JF. Analysis on coordinate conversion error of airborne measuring device. *Optic Precis Eng* 2009; 17: 388–394 (in Chinese).
13. Zhou XY, Ma DX, Fan DP, et al. Error analysis of mast mounted electro-optical stabilized platform based on multi-body kinematics theory. *Proc SPIE* 2011; 7544: 75446R.
14. Waldmann J. Line-of-sight rate estimation and linearizing control of an imaging seeker in a tactical missile guided by proportional navigation. *IEEE T Contr Syst T* 2002; 10: 556–567.
15. Tamhane B, Kurode S and Parkhi P. Novel two-stage observer for line-of-sight rate estimation. *J Guid Control Dynam* 2016; 39: 2586–2593.
16. Sadhu S and Ghoshal TK. Sight line rate estimation in missile seeker using disturbance observer-based technique. *IEEE T Contr Syst T* 2011; 19: 449–454.